PERGAMON

Carbon 38 (2000) 379–395

CARBON

Preparation of activated carbon cloths from viscous rayon. Part II: physical activation processes

F. Rodríguez-Reinoso[a,*], A.C. Pastor[a], H. Marsh[a], M.A. Martínez[b]

[a]*Departamento de Química Inorgánica, Universidad de Alicante, Apartado 99, E-03080 Alicante, Spain*
[b]*INESCOP, P.I. Campo Alto, Elda (Alicante), Spain*

Received 25 January 1999; accepted 1 June 1999

Abstract

Activated carbon cloths were prepared from viscous rayon by a two-step activation process (carbonization followed by activation) and a single-step activation process (simultaneous carbonization and activation), and were compared in terms of gasification rate, development of porosity and changes in breaking strength. Direct activation of the precursor takes place with a higher rate than char activation, the final products of the former process exhibiting slightly lower micropore volume and surface area. The effect of using carbon dioxide or steam as the activating agent was also analyzed, the former producing a continuous development of narrow microporosity and slight widening only above 30% activation, and the latter a widening of micropores as from the early stages of the process.

Keywords: A. Carbon cloth; B. Activation; C. Adsorption; D. Adsorption properties; Mechanical properties

1. Introduction

Porosity in activated carbon cloths is determined by the method of activation used and the precursor material [1–4]. The partial gasification of a char with oxidant gases constitutes the physical (or thermal) activation method, which takes place in two steps [5]. Initially, at activation percentages <10%, the mechanism is the opening of previously inaccessible porosity, the amorphous carbon blocking the char pores being burned-off preferably. With further activation, the carbon of the elementary crystals reacts at different rates in different parts of the surface. Carbon atoms at dislocations, discontinuities and the edges of the elementary crystals, which have unsaturated valences, leave the surface as gaseous oxides. These processes lead in the first stage to new pore formation and in the second stage, at medium and high activations, to widening of the existing pores and formation of larger pores by burn-off of walls between adjacent pores.

The main factors affecting the gasification rate are: (i) active sites concentration in the carbon surface; (ii) carbon crystallinity and structure; (iii) presence of inorganic impurities; and (iv) diffusion of reactive gases to the active sites.

Factors (i) to (iii) depend on the raw material and its previous history. The conditions under which the char has been obtained (carbonization rate, temperature and time) affect its ordination degree and thus, the gasification rate [6,7]. Factor (iv) depends on the material resulting from carbonization (the wider the porosity, the easier it is for diffusion of reacting species and products), and on the conditions of the gasification process, i.e. temperature, flow and kind of activating gas.

Gasification temperature affects gasification rate and this influences porosity development due to a balance between gasification rate and diffusion rate to the inside of the char porosity. The lower the gasification rate, the more uniform will be the extent of the activation process [5]. The literature is not extensive on effects of temperature on the activation process under experimental conditions where other factors are kept constant. For an anthracitic char, a decrease in surface area and pore volumes occurs with increasing temperature of activation by carbon dioxide [8]. For brown-coal [9] and peach stones [10], an independence of surface area with activation temperature was found, being dependent only on the activation percentage.

Berger et al. [9], for a brown-coal char, show that the invariance of surface area with increasing temperature of activation does not contradict anticipated results for the pore volumes. At low activation temperatures, a high

*Corresponding author.

0008-6223/00/$ – see front matter
PII: S0008-6223(99)00118-9

contribution of microporosity was found, but little development of mesoporosity. At higher activation temperatures, microporosity decreased, with a resultant higher proportion of wide micropores (also called supermicropores) and mesopores, these contributing to the surface area, thus compensating for the decrease in loss of narrow microporosity (also called ultramicroporosity). For the peach stones [10], however, increasing temperature of activation led to carbons with slightly higher micropore volumes and much higher mesopores volumes.

Likewise, the activating gas used significantly influences the porosity of the product. Carbon dioxide and steam are the most common agents used. Most studies indicate a higher development of microporosity with carbon dioxide and a more pronounced tendency for widening of porosity with steam [11–14]. There is no unanimous explanation for this behavior, contrary to the one suggested by Wigmans [15], based on the larger size of the carbon dioxide molecule. It is also possible to both carbonize and activate a material in a single stage [10] because of the compatability of carbonizing temperature and temperature of activation.

This work is concerned with the influence of activation conditions on the characteristics of activated carbon cloths obtained from chars as described earlier [7]. The following factors will be examined:

The effect of increasing activation temperature of rayon viscose chars, monitoring changes in porosity and breaking load of resultant carbon cloths, carbon dioxide being the activating gas.

The effect of different activating gases using rayon viscose chars, on development of porosity and breaking strengths of product carbons. Two series, using carbon dioxide and steam, prepared under similar conditions, will be compared.

The effect of different conditions of preparation using rayon viscose chars will be assessed. Activated carbon cloths were prepared by a two-step activation process (carbonization followed by activation), and a single-step activation process (simultaneous carbonization and activation), and compared in terms of gasification rate, development of porosity and changes in breaking strength.

2. Experimental

A segment of viscose rayon cloth, 700×250 mm, was cut from material provided by Moygashel Ltd. (Northern Ireland), composed of identical 100% viscose rayon yarns with a plain weave and a warp and weft density of 9.3 and 8.3 yarns cm^{-1}, respectively. The segment was carbonized in a horizontal furnace at 5°C min^{-1} with a residence time of 2 h at 850°C (char VC^5). It was cut into 50 mm wide strips which were activated as follows: (i) Six strips were activated with carbon dioxide, three at a final temperature of 775°C (series VC^5-C^3), and three at 800°C (series VC^5-C^2). The results for these two series together with those for a series referred as VC^5-C, activated at 825°C (described previously [7]), will establish the effects of temperature of activation. (ii) Five strips were activated with steam (series VC^5-H) at 750°C. The reactivity (rate of gasification) at this temperature was of the same order as that obtained in series VC^5-C. Thus, effects of changes in the activation gas can be studied less ambiguously.

Single-stage activation of ten strips of viscose rayon cloth was carried out: four strips were activated with carbon dioxide at 825°C (V-C), three with carbon dioxide at 800°C (series V-C′), and three with steam at 750°C (series V-H). The effect of using a single-stage activation process can then be studied via a comparison with series VC^5-C and VC^5-H. To facilitate comparison, the nomenclature of all activated carbons (Table 1) will include the overall yield (with respect to the original viscous rayon) instead of the conventional burn-off. In this respect, it is important to note that the yield of carbonization of the viscous rayon to produce char VC^5 is 18.2%.

In the carbon dioxide activation, the heating and cooling processes used carbon dioxide (100 ml min^{-1}). In the steam activation, the furnace was heated initially using a flow of nitrogen (100 ml min^{-1}). A peristaltic pump was connected at 600°C to the system and this introduced a flow of water which vaporized immediately on coming into the furnace to give a flow of steam at 100 ml min^{-1}. At the reaction (activation) temperature of 750°C, the nitrogen was disconnected, the reaction proceeding only with undiluted steam. After the appropriate reaction time, the pump was disconnected and the nitrogen flow restored.

Five TG-DTA experiments were made (TG-DSC92, SETARAM) using char VC^5 (~20 mg). The char was heated at 5°C min^{-1}, under a flow of nitrogen–helium (4:1) at 100 ml min^{-1}, to a final temperature between 750 and 850°C, when the gas mixture was changed to a flow of carbon dioxide–helium (4:1) at 100 ml min^{-1}, and weight loss was monitored against time. From the slope of the weight loss/time graph for the first hour of reaction, the reactivity (gasification rate) at each temperature was calculated.

A further three TG-DTA experiments were carried out, two using the precursor and the other using the char (VC^5), to assess differences between the two-stage and single-stage activation processes. In one the precursor was heated to 900°C under a flow of helium at 80 ml min^{-1}. In the other two experiments the heating of both the precursor and the char took place under a flow of carbon dioxide–helium (1:1) at 160 ml min^{-1}, to a final temperature of 900°C.

Porosity in the activated carbons was assessed by physical adsorption of nitrogen at 77 K and of carbon dioxide at 273 K using automatic equipment (AUTOSORB6, QUANTACHROME), after degasing at 523 K for 5 h. Apparent surface areas (from the BET equation [16] of the nitrogen adsorption data), total micro-

Table 1
Details for activated carbon cloth preparation

Sample	Carb.	Activation				Overall yield (%)
		Temp (°C)	Gas	Time (h)	Activat. (%)	
VC^5-C9	Yes	825	CO_2	2.5	49	9
VC^5-C13	Yes	825	CO_2	1.5	31	13
VC^5-C14	Yes	825	CO_2	1	23	14
VC^5-C16	Yes	825	CO_2	0.5	13	16
VC^5-$C^2$10	Yes	800	CO_2	5.56	45	10
VC^5-$C^2$13	Yes	800	CO_2	3.5	29	13
VC^5-$C^2$15	Yes	800	CO_2	2	19	15
VC^5-$C^3$10	Yes	775	CO_2	8.5	47	10
VC^5-$C^3$12	Yes	775	CO_2	6.1	35	12
VC^5-$C^3$14	Yes	775	CO_2	4	23	14
V-C9	No	825	CO_2	0.3	52	9
V-C11	No	825	CO_2	0.2	42	11
V-C13	No	825	CO_2	0.1	30	13
V-C′9	No	800	CO_2	3	50	9
V-C′12	No	800	CO_2	2	36	12
V-C′13	No	800	CO_2	1.4	29	13
V-C′14	No	800	CO_2	1	21	14
V-C′15	No	800	CO_2	0.6	16	15
VC^5-H7	Yes	750	H_2O	2.1	64	7
VC^5-H10	Yes	750	H_2O	1.5	45	10
VC^5-H13	Yes	750	H_2O	1	31	13
VC^5-H15	Yes	750	H_2O	0.65	19	15
VC^5-H17	Yes	750	H_2O	0.3	10	17
V-H9	No	750	H_2O	0.7	49	9
V-H11	No	750	H_2O	0.45	40	11
V-H14	No	750	H_2O	0.2	26	14

pore total volumes (from the α-method [17], as proposed by Rodríguez-Reinoso et al. [18]), and narrow micropore volumes (from the Dubinin-Radushkevich equation [19] applied to the carbon dioxide adsorption data), were calculated. Mesopore volumes were calculated by subtracting V_α from the volume adsorbed at a relative pressure of 0.95 of the nitrogen adsorption isotherm.

Sample thickness and breaking load were measured as described previously [7].

3. Results and discussion

3.1. Reactivities

Fig. 1 shows the variation of activation percentage with time of reaction at the final temperature for the three series prepared by two-stage activation. The variation is linear indicating that activation took place in a gradual and uniform way, apparently independent of development of porosity. The slopes of the lines, a measure of 'reactivity' of the char, increased with the increasing temperature.

Of the TG curves obtained at five temperatures between 750 and 850°C, the isothermal stage (corresponding to the reaction of the char with the He–CO_2 mixture) has been

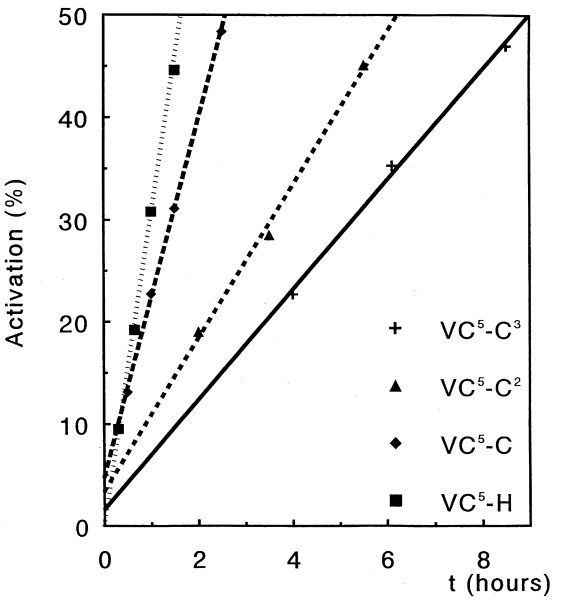

Fig. 1. Activation percentage against residence time (series VC^5-C^3, VC^5-C^2, VC^5-C and VC^5-H).

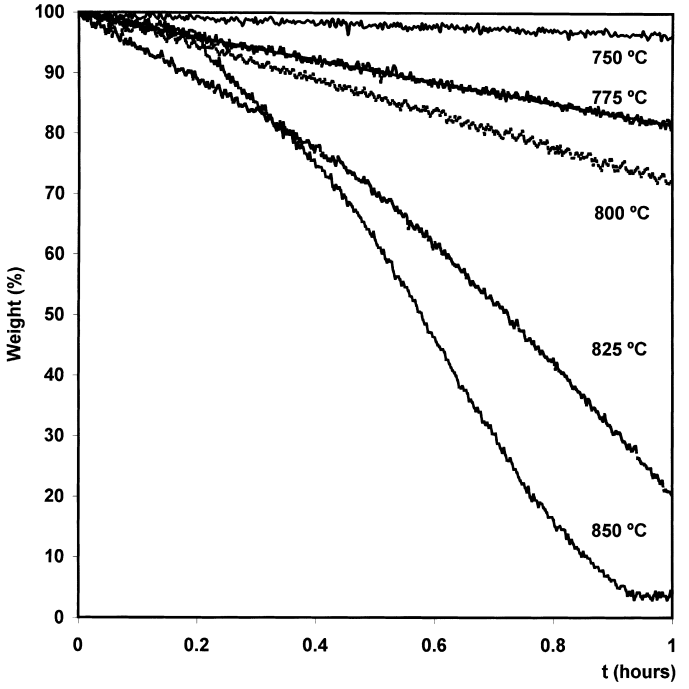

Fig. 2. TG curves for the reaction of char VC[5] with He–CO_2 at different temperatures.

selected and these are as Fig. 2, where weight loss is plotted against time, with reference to the sample weight at the beginning of the isothermal stage. Reactivities at each temperature have been calculated from slopes of initial sections and plotted in Fig. 3 as an Arrhenius diagram. The reactivities obtained in the furnace (for chars with activations <25 wt%, in the three cases) are also shown in Fig. 3. The TG data lie on the same line, 750 to 850°C, providing an apparent activation energy of 260 kJ mol^{-1}. The derived activation energy of 260 kJ mol^{-1} is within the range already described for the carbon-CO_2 reaction [20], but it is somewhat lower than for other chars of different origin [21–23].

The three reactivity values obtained in the furnace plot to give a line of a slightly lower slope than that from the TG data in this temperature range, giving an activation energy of 250 kJ mol^{-1}. The small difference could result from diffusion effects in the furnace because of differences between the experimental methods. For example, the size and weight of sample in the furnace are much larger than in the TG system.

The char gasification rate with steam (calculated from the slope of the activation percentage/residence time plots) is 29.5% h^{-1} at 750°C, being 17.5% h^{-1} in carbon dioxide at 825°C. At a common temperature, the reactivity for the C–H_2O reaction is higher than that for the C–CO_2 reaction, a result which is well-established [12–14,24–27]. Thus, to avoid these effects, two approaches can be adopted: (a) to use dilution of the steam with an inert gas or (b) to use a lower activation temperature. The second approach was used here.

Fig. 4 shows the TG-DTA graphs for the activation of char VC[5]. After a small loss of adsorbed moisture,

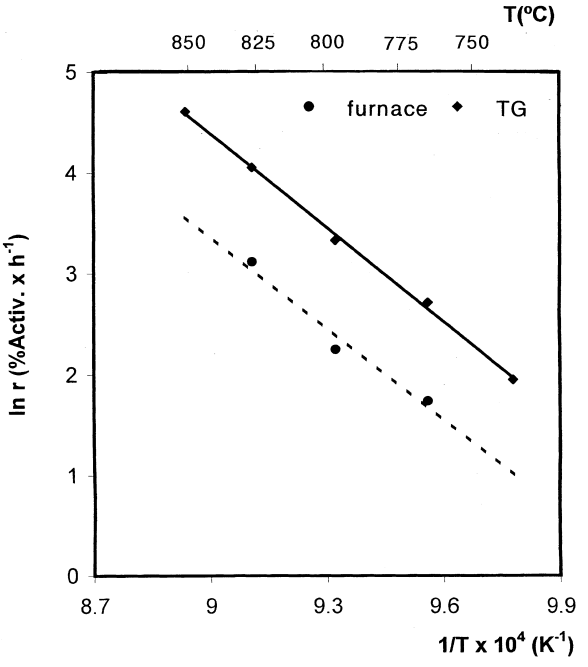

Fig. 3. Arrhenius plots (data obtained in furnace and in TG).

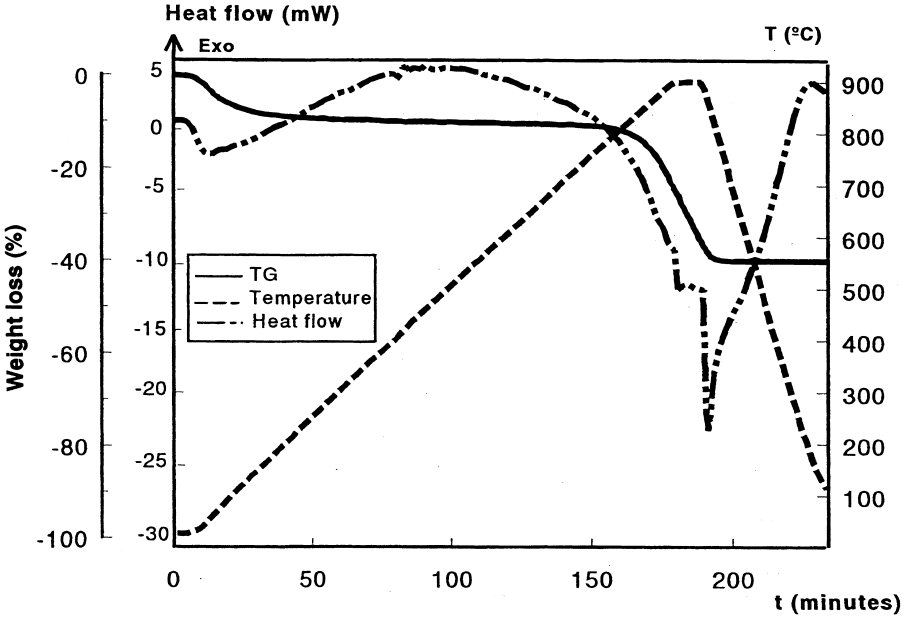

Fig. 4. TG-ATD graph corresponding to the reaction of char VC[5] with He–CO_2.

gasification (as detected by the increase in weight loss) begins at 760°C. Fig. 5, for the viscose rayon precursor, shows a thermogravimetric curve identical to the pyrolytic decomposition of the material obtained using an inert atmosphere (Fig. 6), gasification beginning at ~670°C. The DTA curve shows two endothermic peaks, at about 90°C due to loss of moisture, and at about 900°C, as in Fig. 5, but with a stronger endothermic effect.

The temperature at which the char begins to react with carbon dioxide is thus about 90°C lower using the viscose rayon precursor, the material previously carbonized being more resistant to gasification. There are also differences in

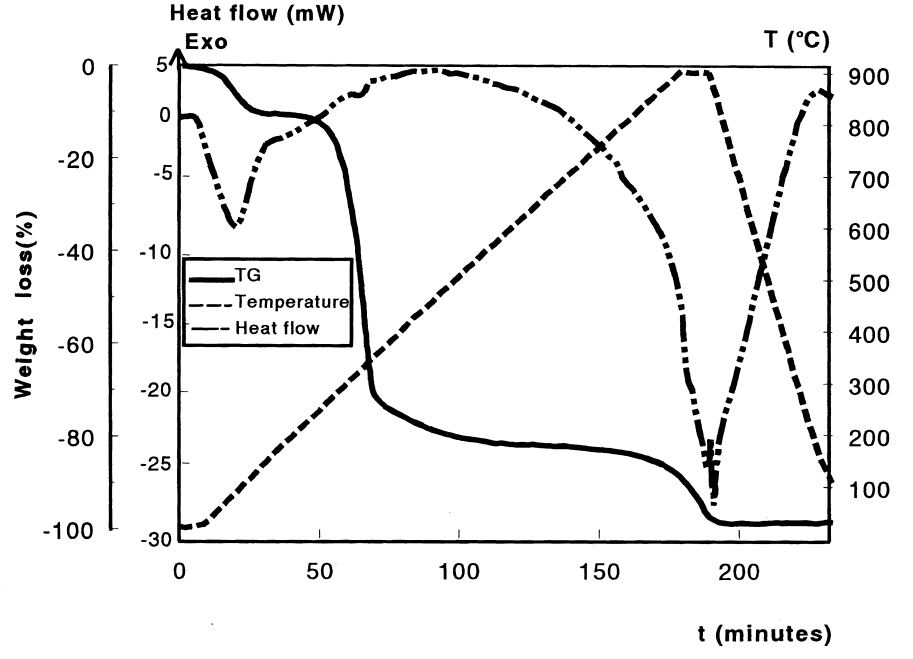

Fig. 5. TG-ATD graph of rayon viscose under He–CO_2 flow.

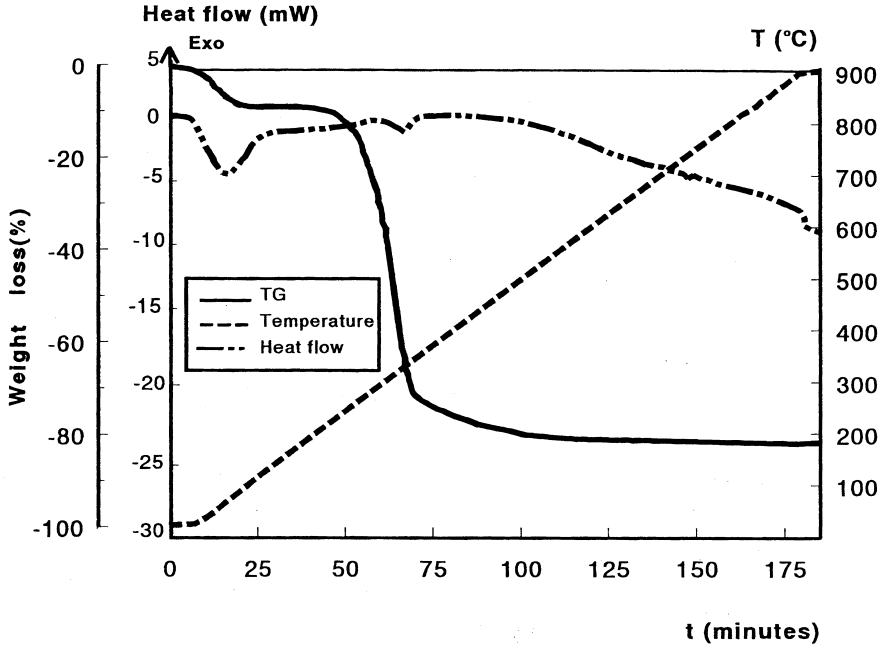

Fig. 6. TG-ATD graph of rayon viscose under He flow.

reactivity at a given temperature. For example, at 825°C the char lost ~2.2 wt% by gasification (corrected for moisture loss). For the rayon precursor, the weight loss at 825°C is ~12 wt%. Fig. 7 shows these differences, the TG curves for both materials (viscose rayon and char) being plotted relative to the weight remaining at 660°C. At this temperature pyrolyses are complete but no gasification has occurred. These differences are to be expected [10]; for (VC^5) this material has been carbonized to a higher temperature (850°C) for 2 h and this leads to a char with a more ordered structure than material V, thus having a lower reactivity.

Fig. 8 shows the overall yields of preparation against the residence time at maximum temperatures for chars of the

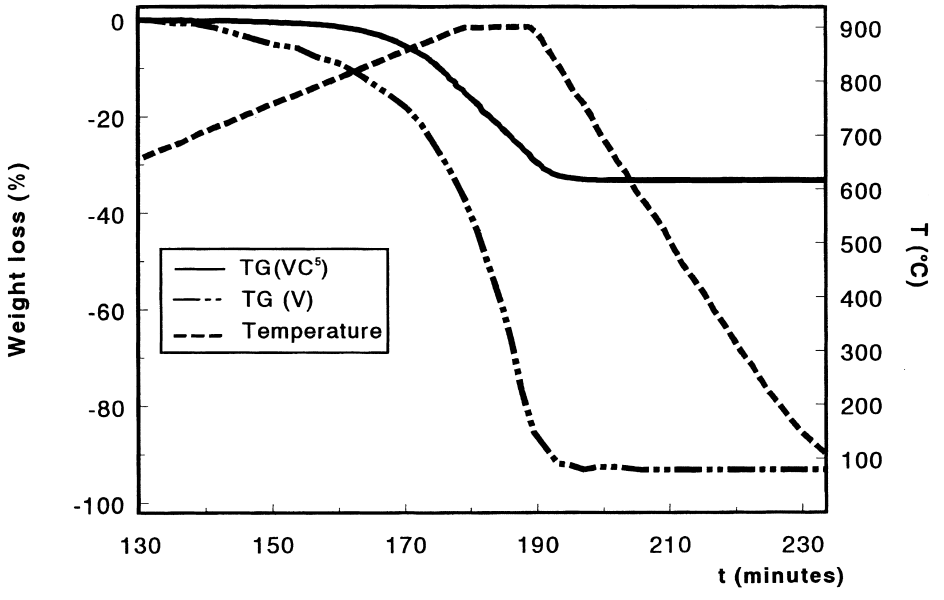

Fig. 7. Comparison between TG curves corresponding to Figs. 4,5.

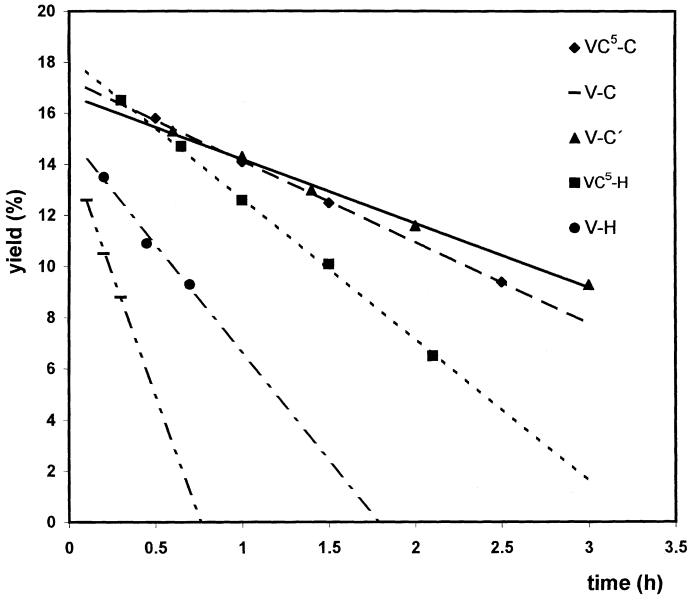

Fig. 8. Evolution of the overall yield with the residence time in the activation stage (series VC^5-C, VC^5-H, V-C, V-C′ and V-H).

three series obtained by direct activation and the two series prepared by two-stage activation (VC^5-C and VC^5-H). For a common activation temperature (825°C for VC5-C and VC; 750°C for VC^5-H and V-H), with both carbon dioxide and steam, the direct process takes place faster than the char activation (as shown in the thermal analyses). For carbon dioxide activation, the gradient of the yield/time line in the direct process is 6 times that of the two-stage activation. This difference is less marked for steam, the factor being only 1.5. Although the lines for the two step procedures intercept the ordinate axis at a yield value near that of the char (18.2 wt%), this does not happen in the direct process, the lines intercepting at a lower value suggesting that at zero time (when the activation temperature was reached), some activation had already taken place. The use of carbon dioxide distinguishes more clearly between the two activation methods because the gas is present during both heating and cooling stages.

The reactivities of carbon dioxide and steam activation are inverted for the direct process, the steam, under this condition, being slower than carbon dioxide, the steam activation temperature being 75°C lower than with carbon dioxide.

3.2. Porosity

Fig. 9 contains the nitrogen adsorption isotherms for carbons of the seven series. All are type I, being typical of microporous solids and have similar shapes. The series obtained by carbon dioxide activation, especially those from the two-stage activation, show increased volumes adsorbed at low relative pressures, some widening of microporosity and little formation of mesoporosity. The series obtained by steam activation show an increase in volumes adsorbed at low relative pressure only to a 19% activation (~15% yield), surpassed which all the isotherms begin from the same value of adsorbed volume. The knee opening (widening of microporosity) and the plateau are additionally more remarkable in these series. The only isotherm showing different characteristics is that of sample VC^5-H7 (64% activation), which must have a considerable proportion of mesopores, from the sharp slope of the plateau and the hysteresis loop. There is no sample of comparable activation extent in the carbon dioxide activated series because of the difficulty in reaching such a high level of activation with this agent without a localized, visible effect in the cloth taking place.

Fig. 10 shows that the adsorptive capacity (expressed as surface area) develops gradually with activation for the chars of the four series prepared by two-stage processes. All the lines intercept the *y*-axis at values higher than that obtained for the char because of the existence on the latter, during adsorption, of activated diffusion by nitrogen [28]. For chars activated with carbon dioxide, the surface area increases with the use of lower activation temperatures, for a common degree of activation, was the same result found in the bibliography [5,8–10]. Initially, steam develops more surface area than does carbon dioxide. However, at high activation levels the tendency is the opposite, the intercept between both lines being at 30% of activation.

The reasons for this low development of surface area by steam at high activation levels are to be seen in Fig. 11, which shows the development of total microporosity (V_α) and narrow microporosity ($V_0(CO_2)$) with activation. Both

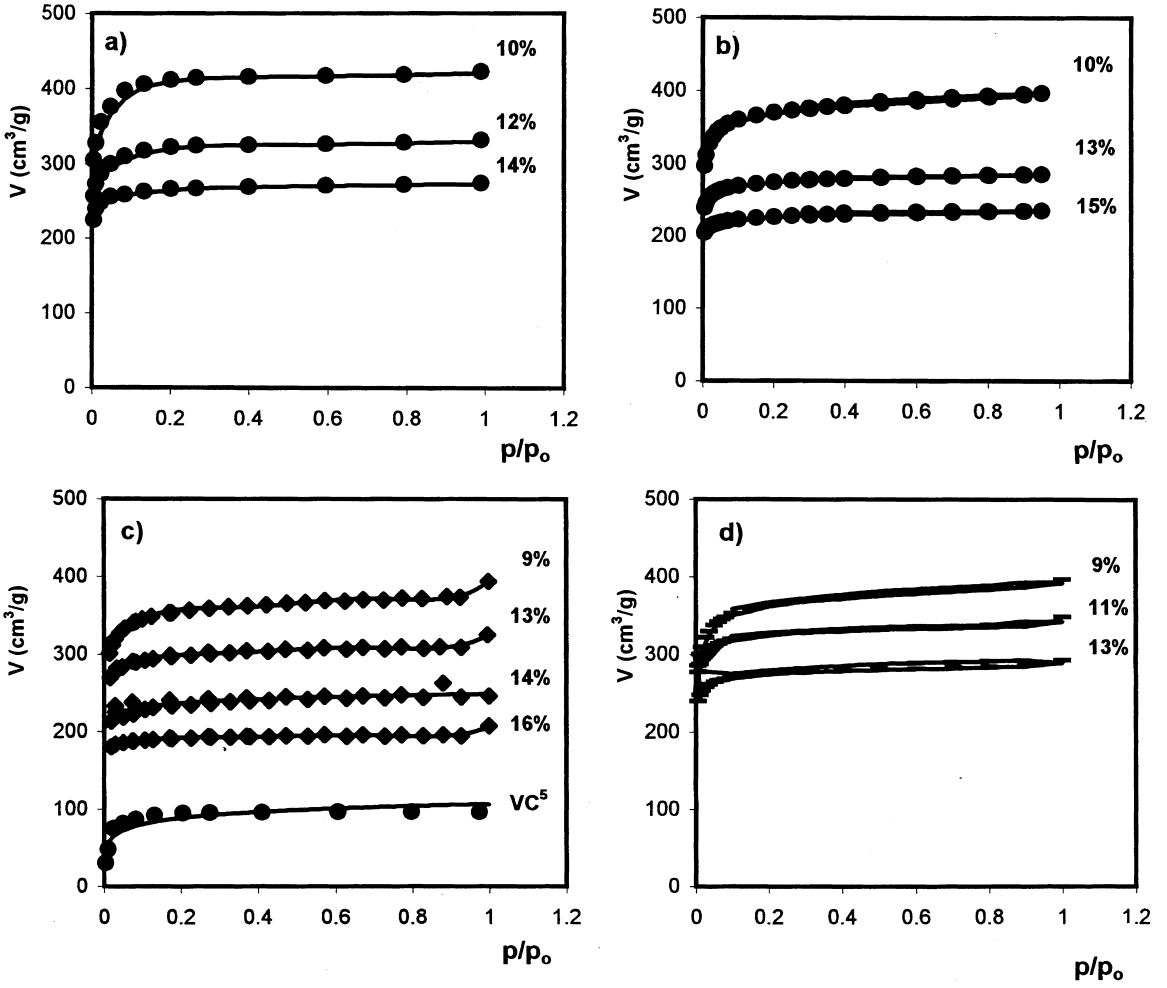

Fig. 9. Adsorption isotherms of nitrogen at 77 K: (a) series VC^5-C^3; (b) series VC^5-C^2; (c) series VC^5-C; (d) series V-C; (e) series V-C′; (f) series VC^5-H; and (g) series V-H.

series (VC^5-C and VC^5-H) have V_α values showing the same tendency of total microporosity to develop in a linearly and parallel way for both series, except for activations>45 wt%, in series VC^5-H, where development of the total microporosity ceases. The line obtained intercepts the *y*-axis at a V_α value higher to the one obtained for the char and is coincident with the $V_0(CO_2)$ value. Although the molecule of carbon dioxide has a similar diameter to that of nitrogen, it is able to be adsorbed simply because of the higher temperature of adsorption, 273 K, compared with 77 K for nitrogen [28].

The most significant difference between both series (VC^5-C and VC^5-H) is with the narrow microporosity (ultramicroporosity), measured by adsorption of carbon dioxide (Fig. 11). Although this value is also developed with activation in both cases, it does so in a more marked way in CO_2 activation, where a line of slope only slightly lower than that for V_α is found. With steam activation, however, although at low activations the $V_0(CO_2)$ value is initially higher compared with that developed by carbon dioxide, it subsequently grows little with further activation. A 54% difference in activation between the least (10%) and most (64%) activated samples of the VC^5-H series shows a $V_0(CO_2)$ increase of only 0.11 $cm^3\ g^{-1}$.

To summarize, although activation by carbon dioxide produces samples with narrow microporosity (ultra-microporosity), steam for activations >30%, leads to a greater development of wide microporosity (super-microporosity), which results in a lower adsorption capacity for these samples when compared with those activated by carbon dioxide.

Fig. 11 shows that with respect to effects of temperature of activation, a decrease in temperature (825°C for series VC^5-C; 800°C for series VC^5-C^2; 775°C for series VC^5-

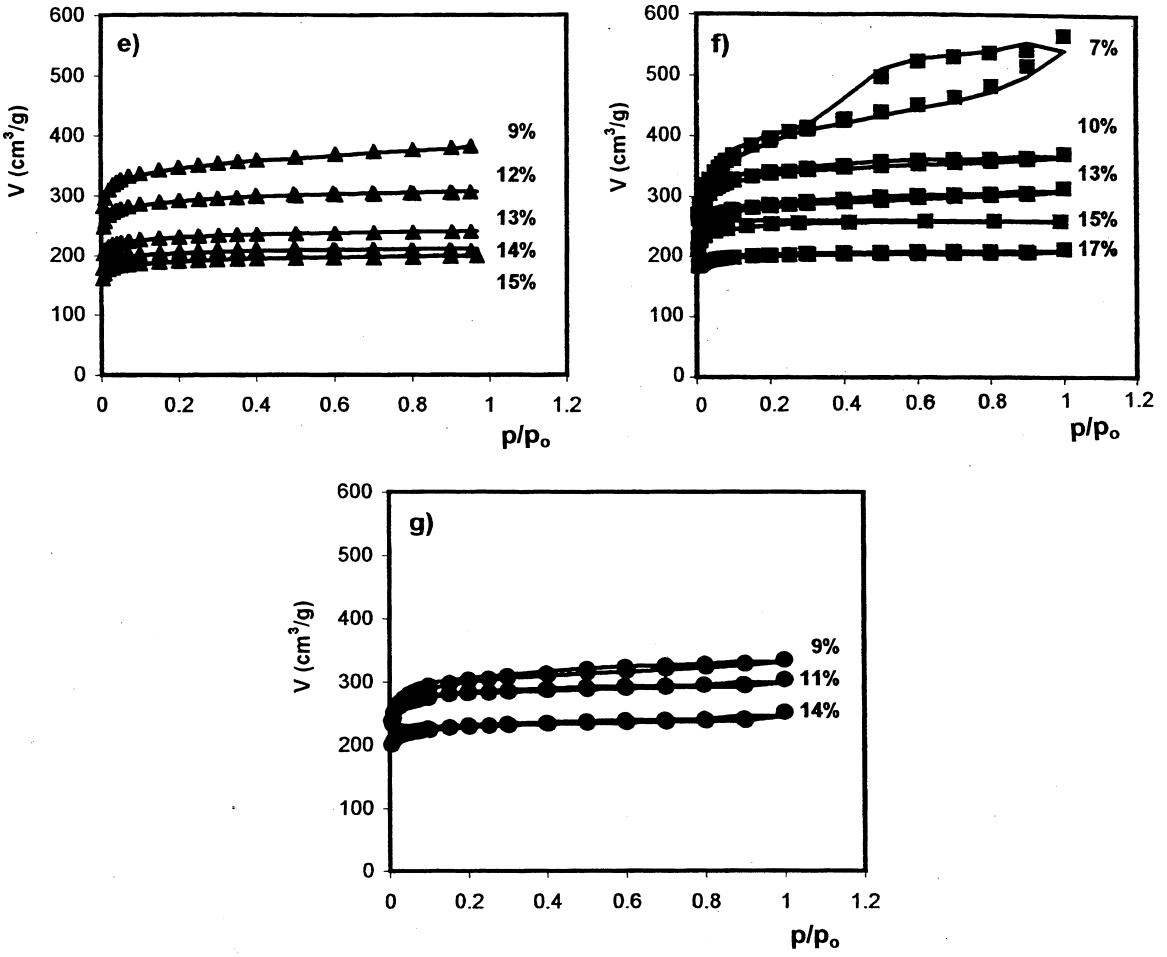

Fig. 9. (*continued*)

C^3) produces an increase in total microporosity (V_α), with a decrease of narrow microporosity ($V_0(CO_2)$), leading to a wider microporosity in samples obtained at lower activation temperatures.

Fig. 12 is a bar diagram for narrow microporosity (ultra-microporosity), wide microporosity (super-microporosity) and mesoporosity in these samples. Volumes of ultra-micropores are higher in samples obtained at higher temperatures. The opposite occurs with super-microporosity, when total microporosity increases with decreasing activation temperature. Carbon dioxide develops little mesoporosity, any notable difference with temperature not being detected, only a lower contribution of mesoporosity to the total porosity being found in samples activated at 775°C.

When carbon dioxide and steam are compared, significant differences in all pore size ranges are seen (Fig. 12). Wide microporosity is not developed by carbon dioxide below a 30% activation, wide microporosity being present at 19 wt% activation with steam. The contribution of this porosity range to total microporosity is 16 and 24% in samples VC^5-H13 (31% activation) and VC^5-H10 (45% activation), respectively, while in samples of comparable activation in series VC^5-C, these percentages are only 6 and 8%. In sample VC^5-H7 (64% activation), there is a decrease in super-microporosity. Here, the nitrogen isotherm indicates a significant mesoporosity not present in other samples. Thus, at activation levels between 45 and 64%, wide microporosity is widened to mesoporosity with steam as the activating agent.

Steam activation occurs initially by creation of ultra-microporosity followed by widening to super-microporosity at activations between 15 and 45 wt% and then widening to mesoporosity at high activations. On the other hand, carbon dioxide activation develops ultra-microporosity continuously during the activation widening to super-microporosity occurring later, from 30% activation.

Fig. 13 is of SEM micrographs showing the physical

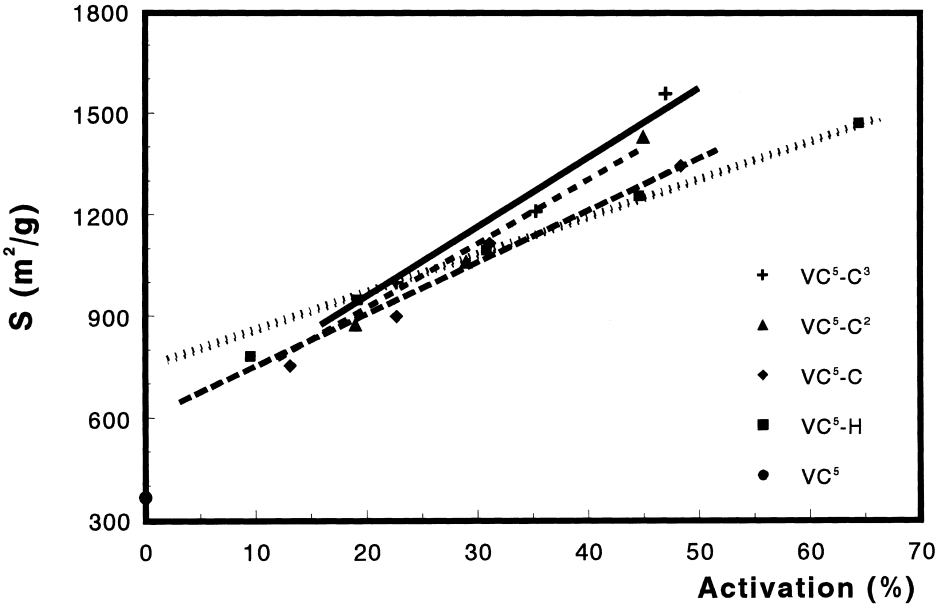

Fig. 10. Evolution of the adsorptive capacity with activation (series VC^5-C^3, VC^5-C^2, VC^5-C, VC^5-H and VC^5).

appearance and structure of the char and two samples from series VC^5-C and VC^5-H which have pronounced differences in porosity. The char fiber shows typical viscose rayon fiber lobular structures, which remain unaltered in the subsequent micrographs, with sample VC^5-H10 (45% activation) showing an abundance of external porosity not observed in fibers activated with carbon dioxide (series VC^5-C).

The activating agent effect (CO_2 or steam) in the porosity development can be summarized. At activations $<$30 wt%, steam develops more surface area, the opposite happening at higher activations. While carbon dioxide activation produces narrow microporosity, in steam activation the microporosity subsequently widens to super-microporosity, mesoporosity and macroporosity, with external burn-off from the fiber surface, as noted previously for other precursors [11–14]. In these experiments, both agents were compared under conditions of similar reactivity, reached by a temperature decrease in steam activation [12,14], or by its dilution with an inert gas [11,13,14]. A higher development of narrow microporosity by carbon dioxide activation and a wider microporosity distribution with steam were found for chars from olive stones [14], isotropic pitch fibers [12,13], and brown coal [11] precursors. Steam also favors widening to mesoporosity, macroporosity and external burn-off at higher activation percentages.

In two of the previous works [13,14], both carbon dioxide and steam developed microporosity gradually and comparably as measured by adsorption of nitrogen, although porosities were higher for samples from carbon dioxide activation, as reported here. However, while the microporosity measured by CO_2 adsorption (narrow microporosity) grew progressively from the value corresponding to the char with carbon dioxide activation, when steam (pure or diluted) was the activating agent, it only grew appreciably in the initial stage of the activation process, reaching a value approximately constant with further activation.

Several suggestions have been put forward to explain the different activating behavior of the two oxidizing agents. Wigmans [25] suggested that the steam molecule, due to its smaller diameter, should be more accessible to smaller pores and concluded that steam activation should develop narrow microporosity more extensively than does carbon dioxide. However, the literature does not support this concept. Yang and Wong [29] consider that the different geometries of the two molecules may be responsible for the activation differences. Carbon dioxide is a linear molecule with a quadrupole, the steam molecule being angular with the oxygen in the middle and having a high dipole moment. Thus, the carbon dioxide molecule maybe more able to penetrate the smaller sizes of microporosity in original carbons. Further suggestions include the role of oxygen surface groups [14,30], the stronger inhibiting effect of reaction product hydrogen compared with carbon monoxide [31], and the higher configurational diffusion of CO_2 in respect to H_2O [32].

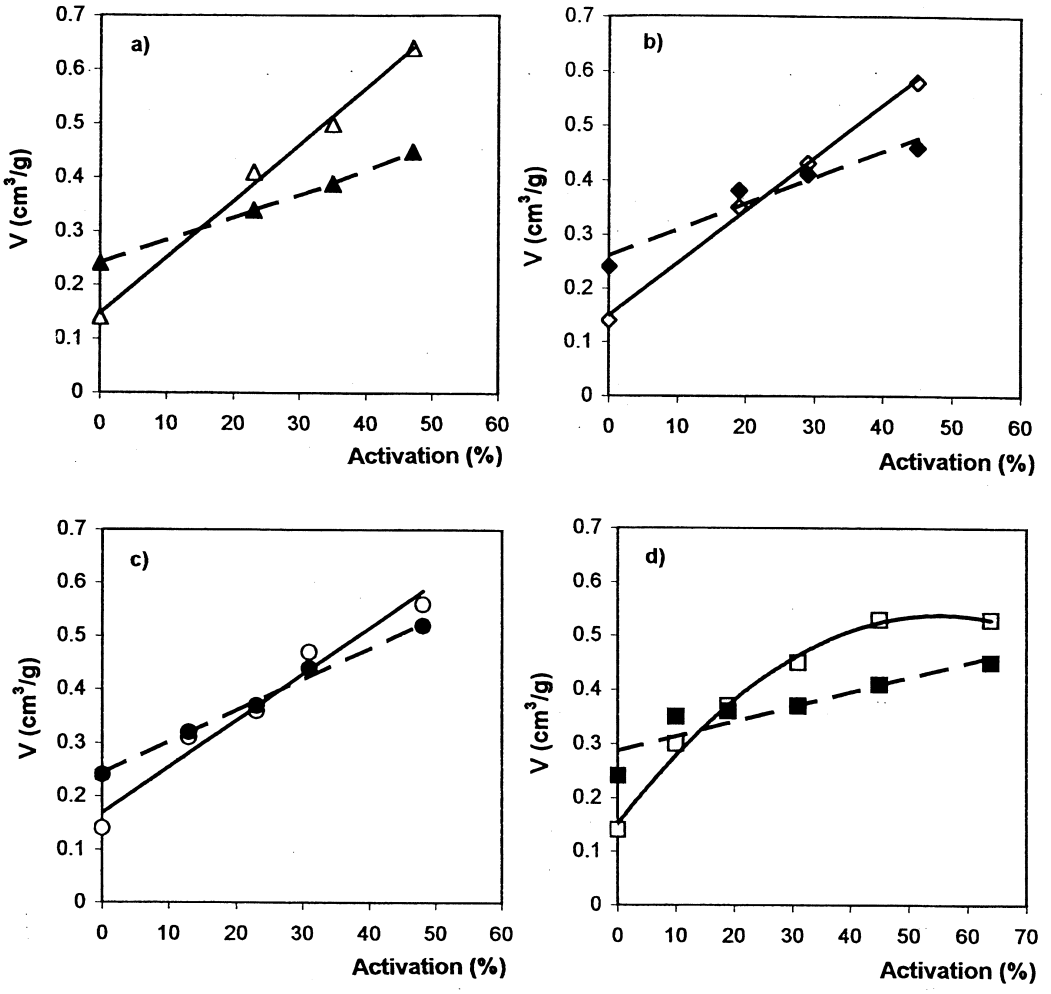

Fig. 11. $V_{\alpha\ (\text{open symbols})}$ and $V(CO_2)$ (solid symbols) against the activation percentage: (a) series VC^5-C^3; (b) series VC^5-C^2; (c) series VC^5-C; and (d) series VC^5-H.

In order to compare direct and two-stage activation, Fig. 14 includes a plot of development of apparent surface area with the overall yield. Considering activation by carbon dioxide, using the direct and two-stage methods, samples of series VC^5-C and V-C have identical adsorptive capacities at equal yields, in agreement with previous works on different lignocellulosic materials [10]. Considering activation by steam, the apparent surface developed more gradually, the plots being parallel for both methods, but the line for the direct process lays below that of the two-stage method.

Fig. 15 shows the evolution of narrow micropore and total micropore volumes with the overall yield. Considering activation by carbon dioxide, using the direct and two-stage methods (series VC^5-C and V-C), samples have identical total microporosities at equal yields, the growth being linear. Considering activation by steam, the total micropore volume developed more gradually, the plots being parallel for both methods, but the line for the direct process lay below that of the two-stage method. More significant differences exist between direct and two-stage activation when comparing narrow microporosity. When considering activation by carbon dioxide, the development of narrow microporosity is slower in the direct process. However, in steam activation, some loss of narrow microporosity occurs. From Fig. 15, it is seen that for both activating gases, direct activation produces lower levels of narrow microporosity.

Fig. 16 is a bar diagram of narrow-, wide- and mesoporosity with the overall yield. There is, for carbon dioxide

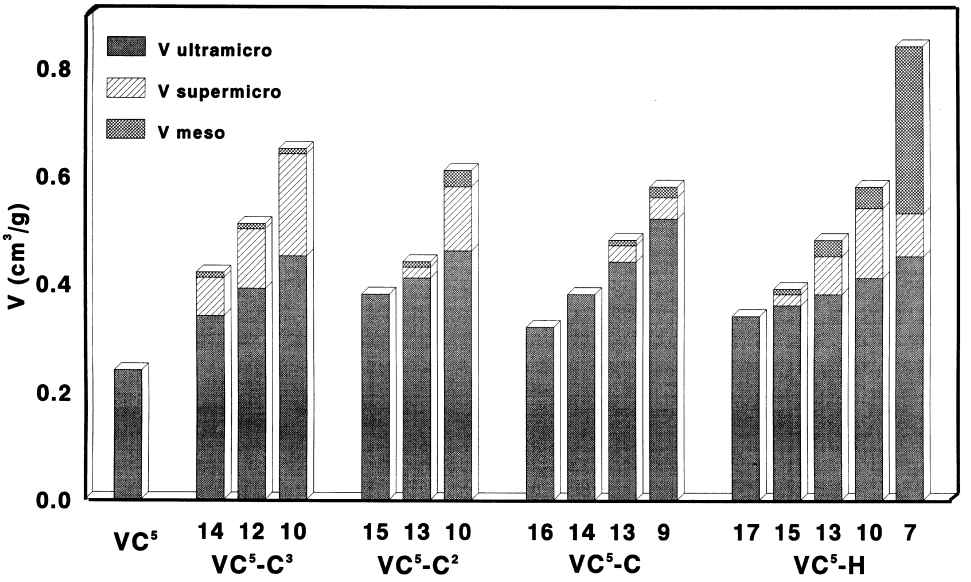

Fig. 12. Ultramicro-, supermicro- and mesopore volumes (two-stage activated samples).

activation, a higher proportion of wide microporosity and mesoporosity in carbons prepared by the direct process. The percentage of wide microporosity and mesoporosity in the total porosity is 7 and 3%, respectively, in samples VC^5-C9 (49% activation) and 18 and 7% in V-C9 (52% activation), confirming the tendency of porosity widening in direct activation. In samples obtained with steam activation, these percentages are closer (21 and 7%, respectively, in VC^5-H10 (45% activation) and 24 and 8% in V-H9 (49% activation). Considering activation by carbon dioxide by the two methods, they show similar total pore volumes (including narrow and wide microporosity and mesoporosity), while for the steam activated samples, lower pore volumes are obtained from direct activation.

When comparing the char activation with the rayon activation at the same temperature, a higher proportion of narrow microporosity results from the two-stage process with a predominance of widening during direct activation. These differences, however, are quite pronounced for carbon dioxide as the activating agent, but are only slight when using steam. This could have two causes. That steam itself produces the effect of porosity widening [11–14] and may mask differences between direct and two-stage activation. The wide difference in gasification rates between both the two processes using carbon dioxide can be explained by the existence of a different balance between gasification rate and diffusion rate inside the porosity [5], and different reaction sites due to the existence of an energy distribution of the active sites. Carbon dioxide may be more able to create microporosity under conditions of low reactivity because of the more shallow gradient of carbon dioxide concentration throughout the material. At higher gasification rates, when the concentration of the product carbon monoxide is higher, that is $[CO]–[CO_2]$, inside the pore, then reaction will be preferred at the external surface of the sample. Lower rates of gasification always promote the development of the more narrow porosity.

To illustrate this latter aspect, a fifth series (V-C′) was obtained by direct activation with carbon dioxide at a lower temperature than used in the two-stage process, to obtain comparable gasification rates (see also Fig. 8). Fig. 14 contains BET surface area data. A development of the adsorptive capacity similar to that in series VC^5-C and V-C is to be seen, but values of the series V-C′ lie slightly under those for the other two series.

The development of the narrow and total micropore volumes (Fig. 15) is similar to the series VC^5-C and V-C, values for the series V-C′ being under those obtained from the two-stage activation by carbon dioxide, again indicating that the microporosity is also mainly narrow in direct activation if series of similar gasification rates are compared, from the parallel evolution of $V(CO_2)$ and V_α, which only differ slightly at high activations.

The volumes of narrow and wide microporosity and mesoporosity for this series are in Fig. 16, showing that the microporosity distribution is similar for both of the carbon dioxide activations (VC^5-C and V-C′), at constant gasification rate. There is a high proportion of narrow microporosity, increasing in volume with activation, unlike the V-C series, and where super-microporosity is not developed until a yield of 12 wt% is reached. The wide microporosity and mesoporosity contents in terms of the total porosity in

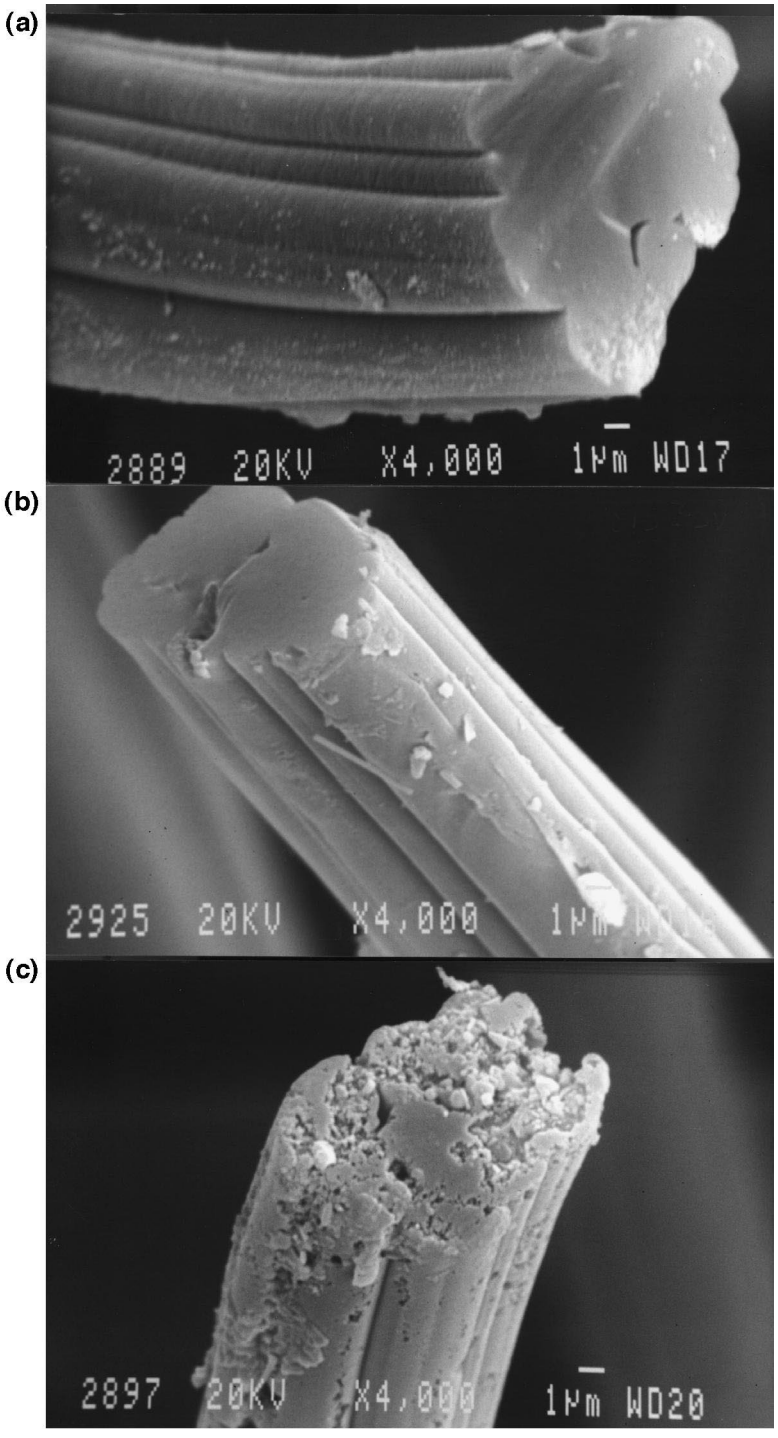

Fig. 13. SEM micrographs of fibers from: (a) char VC^5; (b) VC^5-C13; and (c) VC^5-H10.

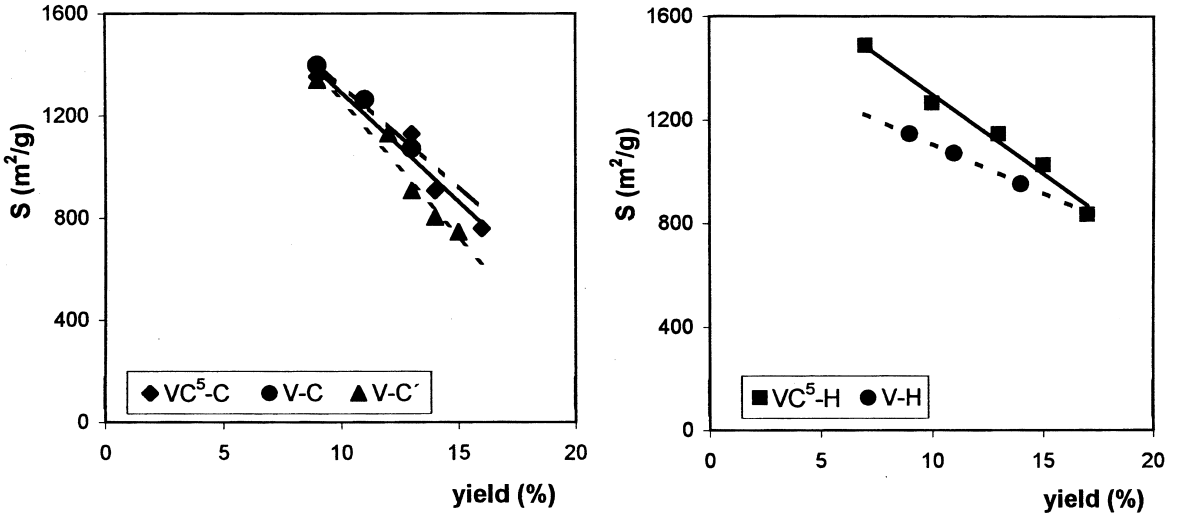

Fig. 14. Evolution of surface area with activation (series VC^5-C, V-C, V-C′, VC^5-H and V-H).

sample V-C′9 (10 and 8%) are similar to those in sample VC^5-C9.

3.3. Strength

Fig. 17 is a plot of cloth thickness and breaking load against yield from the preparation process. The cloth thickness decreases ~38% in the char and the yarn density increases ~33%, due to loss of material and char structure densification and shrinking during carbonization. These values are similar to the longitudinal contraction in the cloth after carbonization (30%). After activation with both agents, the cloth thickness further diminishes slightly, with a roughly linear dependence on extent of activation. With activation by carbon dioxide, the thickness decrease is lower and taking place mainly in the first stages of activation, e.g. being 6% at 11% activation and 8% for 30% activation in series VC^5-C. With steam gasification, it decreases more rapidly, being 16% for 30% activation. This indicates more external burn-off with steam, as also indicated by analyses of the porosity data. Breaking load decreases sharply after carbonization, from 241 to 11.45 N. Changes found in breaking strength with the thermal treatment are similar to a previous study [7], strength decreasing at the beginning of the pyrolysis with a small recovery from ~600°C.

Char strength decreased similarly for the carbon dioxide and steam in the initial stages of activation. Subsequent behavior is different, strength remaining constant to 30% activation with steam and then decreasing although less markedly in the first stages than with carbon dioxide. A comparison of Figs. 11,17 shows a relationship between microporosity and breaking strength. During activation by carbon dioxide, a continuous creation of narrow microporosity accompanies a continuous decrease in breaking strength. For steam activation, porosity widening leads to constancy of microporosity and in breaking strength, as observed for carbon fibers from isotropic pitch [13]. A larger micropore volume in the material indicates the existence of deeper defects in the fiber being detrimental to product strength.

There is no influence of the activation temperature on strength, the values obtained in series VC^5-C^2 and VC^5-C (activated at 800 and 825°C, respectively) being on the same curve. However, samples prepared by direct activation have a higher strength which increases at medium activation percentages associated with densification and shrinkage during carbonization [7]. When using the two-stage method this effect is not observed because of the higher carbonization temperature. In series V-C′, however, the material re-structures and densifies simultaneously with activation, the initial strength increase due to carbonization and later a decrease due to gasification.

4. Conclusions

1. The activation temperature decrease leads to samples with higher adsorptive capacity and micropore volumes, and slightly lower mesopores volumes, because gasification takes place in a slower and more uniform way, and, thus, there is a lower gradient of reactive concentration through the pore. However, a lower development of narrow micropores at the expense of its widening to super-microporosity is found. There is no effect in strength.

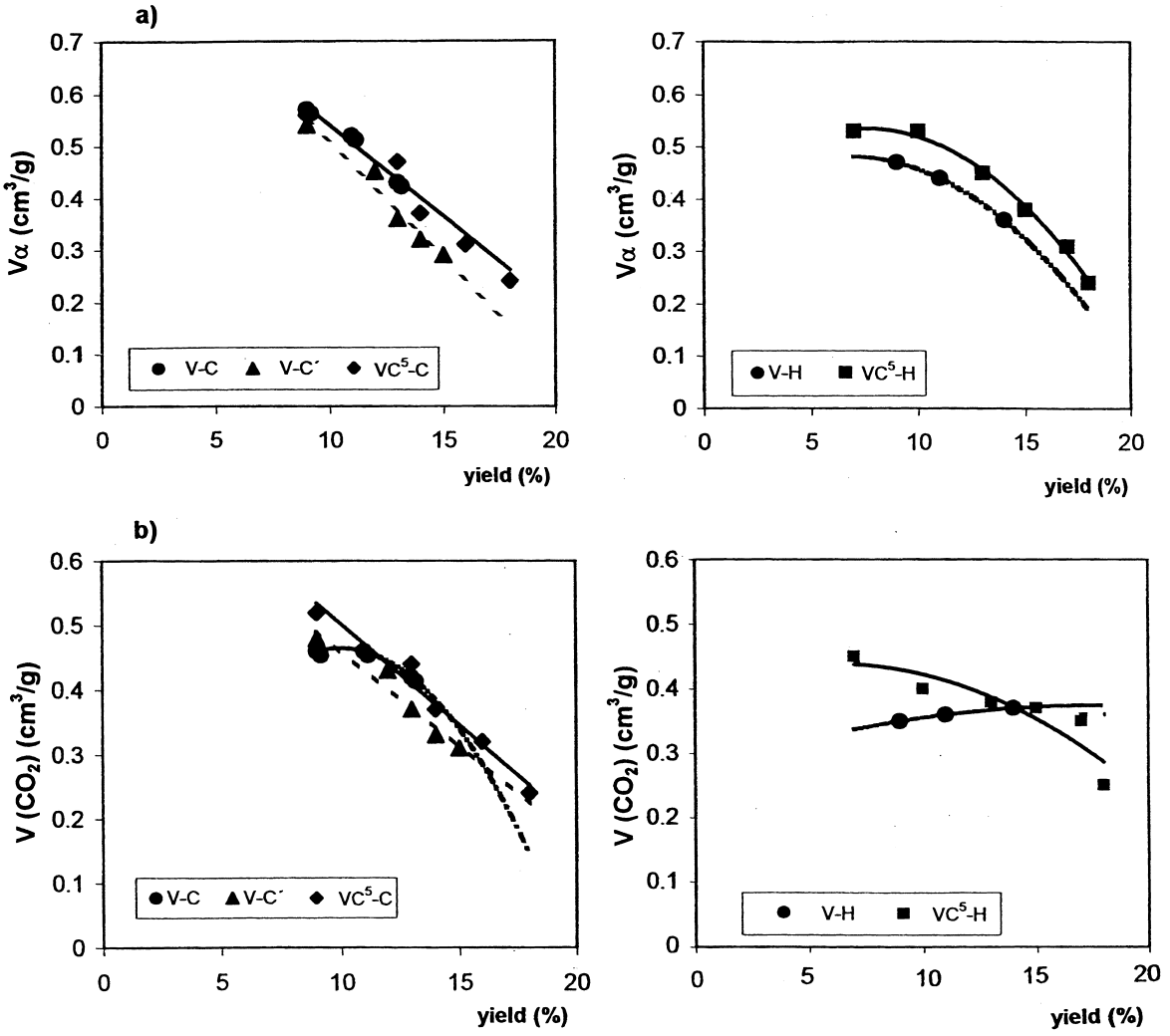

Fig. 15. Evolution with activation of: (a) V_{α} and (b) $V(CO_2)$ (series VC^5-C, V-C, V-C′, VC^5-H and V-H).

2. Carbon dioxide and steam develop their action in a different way during activation. The first one produces a continuous development of narrow microporosity in all the activation stages and a slight widening from 30% activation. Steam, unlike, leads to samples with lower micropore volumes because of its widening to super-microporosity from the beginning of the process. CO_2 produces a higher strength loss during activation due to its higher deepening in narrow micropores.
3. Direct activation of viscose rayon takes place with a higher rate than the char activation, at a given temperature. When series obtained with similar gasification rates are compared, samples of similar characteristics are found with both kind of processes, but a slightly lower surface and micropore development takes place in the direct activation. The strength is preserved in the initial stages of the direct process, because the material is being simultaneously submitted to the carbon structure re-ordination and densification, produced by its carbonization.
4. The breaking load that the cloth is able to stand is low, most of the loss in this magnitude taking place during its carbonization. Thus, a way of improving this parameter must go through the modification of the carbonization process.

Acknowledgements

ACP acknowledges a fellowship from the Spanish Ministry of Education and Science. Financial support was

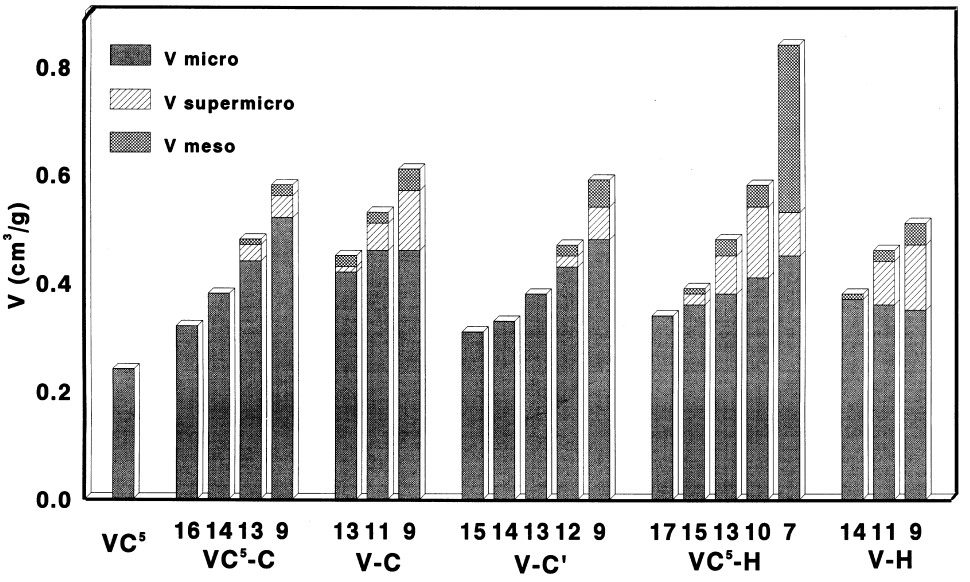

Fig. 16. Ultramicro-, supermicro- and mesopore volumes (series VC^5-C, V-C, V-C′, VC^5-H and V-H).

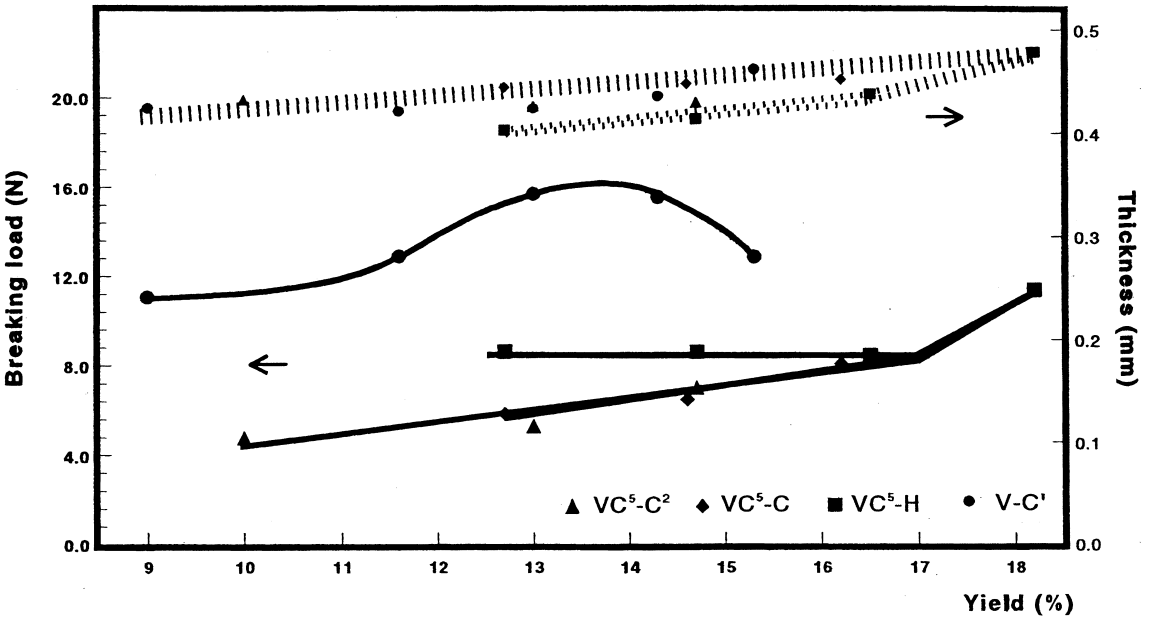

Fig. 17. Evolution with activation of cloth thickness and breaking load.

received also through the project DGICYT PB94-1500. H.M. thanks the Spanish DGICYT (SAB95-0086).

References

[1] Capon A, Freeman JJ, McLeod AI, Sing KSW. In: Proceedings of London Int. Carbon & Graphite Conf, London: Soc. of Chemical Industry, 1982, p. 154.
[2] Carrott PJM, Freeman JJ. Carbon 1991;29:499–506.
[3] Freeman JJ, Tomlinson JB, Sing KSW, Theocharis CR. Carbon 1993;31:865–9.
[4] Tomlinson JB, Freeman JJ, Sing KSW, Theocharis CR. Carbon 1995;33:789–94.
[5] Rodríguez-Reinoso F. In: Lahaye J, Ehrburger P, editors, Fundamental issues in control of carbon gasification reactivity, Netherland: Kluwer Academic Publishers, 1991, pp. 553–65.
[6] Brunner PH, Roberts PV. Carbon 1980;18:217–24.

[7] Pastor AC, Rodríguez-Reinoso F, Marsh H, Martínez MA. Carbon, in press.
[8] Walker PL. In: Figueiredo JL, Moulijn JA, editors, Carbon and coal gasification, Netherland: Martinus Nijhoff, 1986, pp. 1–23.
[9] Berger J, Siemieniewska T, Tomkov K. Fuel 1976;55:9.
[10] Rodríguez-Reinoso F, Martín-Martínez JM, Molina-Sabio M, Pérez-Lledó I, Prado-Burguete C. Carbon 1985;23:19–24.
[11] Tomkov K, Siemieniewska T, Czechowski F, Jankowska A. Fuel 1977;56:121.
[12] Ryu SK, Jin H, Gondy D, Pusset N, Ehrburger P. Carbon 1993;31:841–2.
[13] Alcañiz-Monge J, Cazorla-Amorós D, Linares-Solano A, Yoshida S, Oya A. Carbon 1994;32:1277–83.
[14] Rodríguez-Reinoso F, Molina-Sabio M, González MT. Carbon 1995;33:15–23.
[15] Wigmans T. In: Figueiredo JL, Moulijn JA, editors, Carbon and coal gasification, Netherland: Martinus Nijhoff, 1986, pp. 559–99.
[16] Brunauer S, Emmett PH, Teller E. J Am Chem Soc 1938;60:309.
[17] Sing KSW. Chem Ind 1968;:1520.
[18] Rodríguez-Reinoso F, Martín-Martínez JM, Prado-Burguete C, McEnaney B. J Phys Chem 1987;91:515–6.
[19] Dubinin MM, Radushdevich LV, Zaverina ED. Ah Fiz Khim 1947;21:1351.
[20] Kapteijn F, Moulijn JA. In: Figueiredo JL, Moulijn JA, editors, Carbon and coal gasification, Netherland: Martinus Nijhoff, 1986, p. 291.
[21] Radovic LR, Steczko K, Walker PL, Jenkins RG. Fuel Processing Technology 1985;10:311.
[22] Capon A, Maggs FAP. Carbon 1983;21:75–80.
[23] DeGroot WF, Shafizadeh F. Fuel 1984;63:210.
[24] Linares-Solano A, Mahajan OP, Walker PL. Fuel 1979;58:327.
[25] Wigmans T. Carbon 1989;27:13–22.
[26] Lin GQ, Do DD. Carbon 1992;30:21–30.
[27] Kühl H, Kashani-Motlagh MM, Mühlen HJ, VanHeek KH. Fuel 1992;71:879.
[28] Rodríguez-Reinoso F, Linares-Solano A. In: Thrower PA, editor, Chemistry and physics of carbon, vol. 21, New York: Marcel Dekker, 1988, pp. 1–146.
[29] Yang RT, Wong C. J Catal 1983;82:245.
[30] Molina-Sabio M, González MT, Rodríguez-Reinoso F, Sepúlveda-Escribano A. Carbon 1996;34:505–10.
[31] Walker PL. Carbon 1996;34:1297–9.
[32] Alcañiz-Monge J, Cazorla-Amoros D, Linares-Solano A. Carbon 1997;35:1665–8.